


# Optimization Method for Practical Design of Planar Arbitrary-Geometry Thermal Cloaks Using Natural Materials

Fu-Yao Yang, Fu-Sui Hung, Woon-Shing Yeung, and Ruey-Jen Yang<sup>✉\*</sup>  
*Department of Engineering Science, National Cheng Kung University, Tainan, Taiwan*

 (Received 22 October 2020; revised 23 December 2020; accepted 15 January 2021; published 3 February 2021)

This study proposes an optimization method for the design of planar arbitrary-geometry thermal cloaks using natural materials based on the bilayer theory in thermal-cloaking studies. Our objective is to provide a practical design method for bilayer thermal cloaks of arbitrary shapes by determining the optimal outer-layer conductivity of the bilayer yielding the best thermal-cloaking performance. The method accounts for a potentially conducting inner layer, which is deemed more realistic from a practical standpoint as opposed to an ideal bilayer having a perfectly insulated inner layer. The proposed method is applied to solve thermal-cloaking problems involving not only conventional circular and elliptical geometries but also arbitrary-geometry thermal cloaks, as well as nonlinear background temperature distributions. For the ideal circular and elliptical bilayer cloaks, the proposed method yields the same analytical results as reported in the literature. For those cases where an analytical solution is not known to exist, the results demonstrate that excellent thermal-cloaking performance can be achieved on the basis of the bilayer design using the optimal outer-layer conductivity determined from the optimization method for a given set of background, inner-layer, and cloaked-region conductivities.

DOI: [10.1103/PhysRevApplied.15.024010](https://doi.org/10.1103/PhysRevApplied.15.024010)

## I. INTRODUCTION

As the semiconductor industry continues to advance, increasing transmission rates and the persistent trend toward device miniaturization have resulted in a dramatic increase in the heat-flux density of electronic components. The reliability and performance of such components are critically affected by the temperature, and hence the need for effective thermal-management techniques has emerged as a pressing concern in recent decades. To this end, thermal cloaking plays a potentially significant role in thermal management of electronic systems and protection of the components within them [1].

By adaption of the theory of invisible cloaks for electromagnetic waves based on transformation optics [2,3], thermal-cloak proposals for steady-state conduction were first given in Refs. [4,5] and were later extended to transient heat conduction in Ref. [6]. Historically, design of thermal cloaks may be performed using either transformation thermodynamics or bilayer theory. The former method leads the use of heterogeneous and anisotropic thermal metamaterials. However, metamaterials are seldom found in nature and cannot be easily made. Consequently, the feasibility of fabricating thermal cloaks using composite natural materials has attracted great interest in the recent literature [7–9].

The bilayer theory [10], on the other hand, considers a thermally insulated inner layer and a thermally conductive outer layer, where both layers are made of homogeneous natural materials. Analytical solutions have been obtained for a circular (spherical) bilayer thermal cloak and a confocal elliptical (ellipsoidal) bilayer thermal cloak [10,11], and were verified both numerically and experimentally. Variants of the bilayer thermal cloak have been proposed, mainly to ease the constraint on the high conductivity ratio of the outer layer and the background imposed in bilayer theory, thus simplifying the task of selecting natural materials for its implementation [12,13]. A bilayer carpet thermal cloak based on natural bulk materials for the cloaking of objects with semicircular and semielliptical geometry is described in Ref. [14].

The problem of planar thermal cloaks with arbitrary shapes and general background temperature fields has been analytically solved by transformation thermodynamics [6]. In contrast, an analytical bilayer solution is available only for circular and confocal elliptical geometry, with a linear background temperature distribution. Thus, the objective of this study is to develop a general method for the design of planar bilayer thermal cloaks of arbitrary shapes and with a general background temperature distribution. The primary result of the proposed method is the optimal conductivity for the outer layer, which gives the best-possible thermal-cloaking performance of the given physical system. The method can be applied to a minimally

\*rjyang@mail.ncku.edu.tw

conducting inner layer, which is more realistic from a practical standpoint.

## II. THEORETICAL ANALYSIS AND METHOD

### A. Brief review of existing theory

It is well known that transformation thermodynamics (see, e.g., Ref. [6]) yields the following conductivity tensor for the transformed medium:

$$\underline{\underline{\kappa'}} = \frac{\mathbf{J}\mathbf{a} \cdot \kappa \cdot \mathbf{J}\mathbf{a}^T}{\det \mathbf{J}\mathbf{a}}, \quad (1)$$

where  $\mathbf{J}\mathbf{a} = \frac{\partial(x',y',z')}{\partial(x,y,z)}$  is the Jacobian matrix from  $(x, y, z)$  to  $(x', y', z')$ . Design of thermal cloaks based on transformation thermodynamics is thus reduced to design of thermal metamaterials having the transformed conductivity shown in Eq. (1).

The bilayer theory, based on a perfectly insulated inner layer, yields the following outer-layer conductivity for a circular cloak [10]:

$$\kappa = \frac{R_3^2 + R_2^2}{R_3^2 - R_2^2} \kappa_b, \quad (2)$$

where  $R_2$  and  $R_3$  are the inner-layer radius and the outer-layer radius, respectively, and  $\kappa$  and  $\kappa_b$  are the thermal conductivities of the outer layer and the background, respectively. The corresponding solution for an ideal elliptical bilayer thermal cloak when the background heat flux is in the  $x$  direction is given by [11]

$$\kappa = \tanh \xi_2 \coth(\xi_2 - \xi_1) \kappa_b, \quad (3)$$

where  $\xi_1$  and  $\xi_2$  are bounding confocal ellipses for the outer layer.

### B. Optimization method

In general, thermal-cloaking analyses use the forward approach, in which the temperature field is determined on the basis of given thermal properties. By contrast, inverse problems aim to calculate unknown information from known results. Notably, even if the problem considered has no analytical solution, which is the case for an arbitrary-shaped bilayer cloak, the best solution (i.e., the solution that yields the best performance relative to some predefined criteria) can still be found. This inverse approach has been successfully applied to deduce the transformed anisotropic conductivity coefficients, Eq. (1), for a circular thermal cloak [15]. In general, inverse heat-conduction problems involve deducing unknown material parameters (in our case, the thermal conductivity of the outer layer in a bilayer thermal cloak) from known data (in our case, the given background temperature distribution).

A practical challenge of the bilayer design is the inner layer; it is difficult to find materials that are perfectly insulated. Hence, the requirement imposed on the inner layer of the bilayer cloak in the analytical solutions described above [Eqs. (2) and (3)] is almost impossible to achieve. Accordingly, to extend the practicality of bilayer-thermal-cloak design, the present method accounts for a realistically conducting inner layer. As an example, the inner layer could be constructed of polydimethylsiloxane, which has a thermal conductivity of about 0.15 W/mK. The proposed method combines the bilayer theory and an optimization method based on the inverse perspective to determine the optimal conductivity of the outer layer (unknown in our method), which results in a thermal-cloaking performance closest to that of an ideal cloak.

Figure 1 illustrates the inverse problem considered in the present study, where Fig. 1(a) shows the pure-background region (i.e., no cloak), while Fig. 1(b) shows the background region with the addition of the bilayer thermal cloak.

The external-temperature-field distributions  $T^e$  and thermal conductivity of the inner layer  $\kappa_2$  are specified. The left and right boundaries of the computational domain are assumed to be at a high temperature  $T_H$  and a low temperature  $T_L$ , respectively. The upper and lower boundaries are adiabatic. The conductivity of the background is represented by  $\kappa_b$  and that of the inner layer is represented by  $\kappa_2$ . The objective is to achieve the ideal condition of  $T_i^e = T^e$  as much as possible through the selection of a material with an appropriate thermal conductivity  $\kappa$  as the outer layer.

A cost function  $J$ , adopted from Ref. [15], of the corresponding optimization problem is formulated as

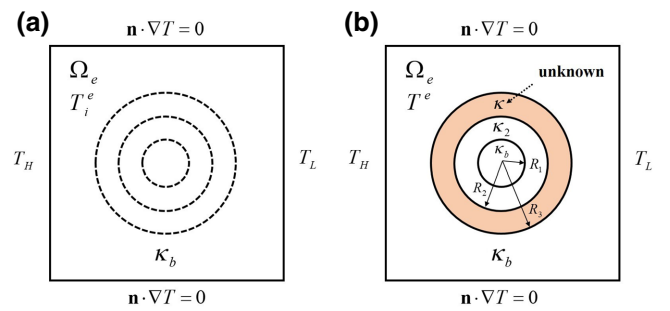


FIG. 1. (a) Pure background (object not protected by a thermal cloak). (b) Bilayer thermal cloak, in which  $0 \leq R \leq R_1$  is a protected region,  $R_1 \leq R \leq R_3$  is a bilayer natural-homogeneous-material region, and  $R_1 \leq R \leq R_2$  is a thermally-insulating-material region. In addition,  $\Omega_e$  is an external region and  $T_i^e$  is the external temperature field of the pure background (without obstacles), in which superscript  $e$  denotes the external region and subscript  $i$  denotes the physical state of the pure background.  $T^e$  is the external temperature field of the background in the presence of an obstacle (i.e., thermal cloak).

$$J = \sum_{n=1}^N (T_n^e - T_{i,n}^e)^2, \quad (4)$$

where  $n$  is the  $n$ th node of the mesh points and  $N$  is the total number of nodes in the outer region  $\Omega_e$ .

Equation (4) ensures that the background temperature field is minimally impacted when the optimal outer-layer conductivity is found. Mathematically, Eq. (4) represents the mean square error of fulfilling the cloaking requirement of no impact on the background temperature distribution. As such, the minimum value of the cost function gives the highest cloaking performance [15]. Since the inner layer is anticipated to be conducting in the practical design of bilayer thermal cloaks, the condition of a uniform temperature distribution in the cloaked region (i.e., region bounded by the inner layer) is theoretically impossible. In this regard, the extent of the impact on the background thermal field is indeed a suitable measure of cloaking effectiveness.

For a bilayer thermal cloak, the cost function,  $J$ , is a function of the outer-layer conductivity,  $\kappa$ , only. The present study seeks a solution of  $\kappa$  such that the derivative of  $J$ ,  $J' = dJ/d\kappa = 0$  (i.e., the best value of  $\kappa$  approximating the thermal-cloaking effect). For each value of  $\kappa$  considered, the steady-state heat-conduction equation is solved to find the corresponding  $T^e$ . In the present study, the zero point of the first-derivative curve (i.e., the root of the equation  $J' = 0$ ) is obtained iteratively with use of the secant method, [16]; that is,

$$\kappa_{n+1} = \kappa_n - J'(\kappa_n) \left[ \frac{\kappa_n - \kappa_{n-1}}{J'(\kappa_n) - J'(\kappa_{n-1})} \right]. \quad (5)$$

$J'$  is evaluated with use of a typical center-difference approximation.

The performance of the secant method is critically dependent on the choice of initial values. In particular, if the two initial values ( $\kappa_0, \kappa_1$ ) are far from the best solution, the computing time increases. Here we propose an effective-area approximation of the analytical solution, Eq. (2), to estimate the initial guess. Thus, Eq. (2) can be rewritten as

$$\kappa = \frac{\pi R_3^2 + \pi R_2^2}{\pi R_3^2 - \pi R_2^2} \kappa_b = \frac{A_3 + A_2}{A_3 - A_2} \kappa_b. \quad (6)$$

Equation (6) can be regarded as the ratio of two areas,  $A_2$  and  $A_3$ , where  $A_2 = \pi R_2^2$  and  $A_3 = \pi R_3^2$ . Figure 2 illustrates the effective-area concept. Notably, when one is solving the arbitrary-shaped-bilayer-thermal-cloak problem, Eq. (6) provides the means to transform the area of the required cloak to that of an equivalent circular bilayer cloak. The equivalent-area ratio [Eq. (6)] can thus be used to determine an initial estimate of the thermal conductivity of the outer layer,  $\kappa_e$ . The two initial guesses ( $\kappa_0, \kappa_1$ ) are then specified around this initial estimate,  $\kappa_e$ .

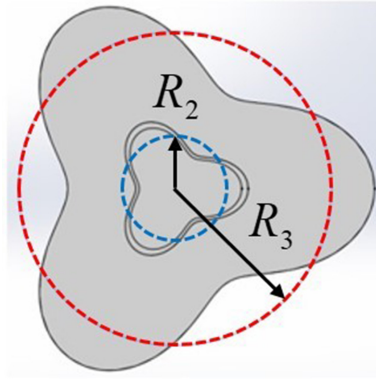


FIG. 2. Illustration of the equivalent-area formula. The actual inner area and outer area are equivalent to circles with radii  $R_2$  and  $R_3$ , respectively.

The optimization process is implemented by our coupling COMSOL Multiphysics [17] to a calculation platform (we use MATLAB [18]). The main steps in the optimization procedure consist of importing the necessary COMSOL Multiphysics output files into MATLAB and performing the necessary iteration in MATLAB to arrive at the optimal outer-layer conductivity such that the cost function  $J$  is minimized.

### III. RESULTS AND DISCUSSION

To verify the accuracy of the optimization program described above, the optimal solutions obtained for a circular bilayer cloak and for an elliptical bilayer cloak are compared with the analytical solutions presented in Refs. [10,11] based on bilayer theory. For both methods, the thermal-conductivity ratio  $\kappa_2/\kappa_b$  is used to quantify the degree of insulation provided by the inner layer of the cloak. In addition, the difference between the optimized result and the ideal solution is quantified by the metric  $\eta = |(\kappa_{\text{opt}} - \kappa_{\text{bl}})/\kappa_{\text{bl}}|$ , where  $\kappa_{\text{opt}}$  is the optimal outer-layer conductivity obtained from the proposed method and  $\kappa_{\text{bl}}$  is the corresponding ideal solution given in Refs. [10,11]. The performance of the thermal cloak is evaluated with use of the temperature deviation  $\lambda = \sqrt{J_{\text{min}}/N}$  as a figure of merit (FOM), where a value of  $\lambda \rightarrow 0$  indicates a cloaking performance closer to that of an ideal thermal cloak.  $\lambda$  is an average value that describes the “overall” cloaking performance over the entire external area rather than the “local” performance. In addition,  $J_{\text{min}}$  is the minimum cost-function value under the optimal solution ( $\kappa_{\text{opt}}$ ) and  $N$  is the total number of nodes in the outer region  $\Omega$ .

For all cases considered herein, the background is taken as a  $150 \times 150 \text{ mm}^2$  region with a linear temperature distribution having  $T_H = 353 \text{ K}$  and  $T_L = 293 \text{ K}$ , as shown in Fig. 1. Also, the background conductivity is taken to be the same as that for the cloaked region (i.e., region

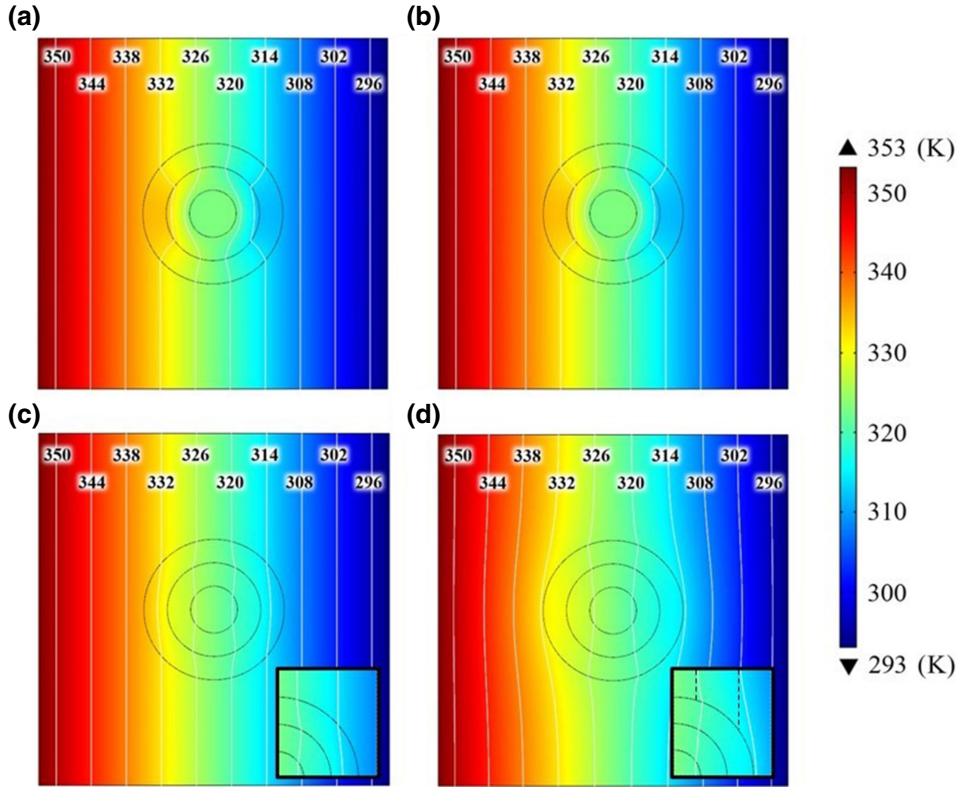


FIG. 3. Simulated temperature distributions around a circular bilayer thermal cloak.  $R_1 = 10$  mm,  $R_2 = 20$  mm, and  $R_3 = 30$  mm (a) Present result:  $\kappa_2 = 0.001$  W/mK and  $\kappa_{\text{opt}} \approx 25.99$  W/mK. (b) Ideal-bilayer theory [10]:  $\kappa_2 \approx 0$  W/mK and  $\kappa = 26$  W/mK. (c) Present result:  $\kappa_2 = 1.5$  W/mK and  $\kappa_{\text{opt}} \approx 0.79$  W/mK. (d) Ideal-bilayer theory [10]:  $\kappa_2 \approx 0$  W/mK and  $\kappa = 2.6$  W/mK. White lines show isotherms and corresponding temperatures. The region indicated in the inset in (d) shows obvious distortion of isotherms. Dashed black lines show the ideal cloaking isotherms.

enclosed by the inner layer). Figure 3 shows the numerical results for a circular bilayer obtained by the present optimization method and by direct simulation using the ideal analytical solution, Eq. (2). Table I summarizes the analyzed parameters and results. As expected, for the case where the inner-layer conductivity is 0.001 W/mK, the present method yields an optimal outer-layer conductivity in close agreement with the analytical value based on Eq. (2). Both the optimized results and the analytical results show perfect cloaking, Figs. 3(a) and 3(b).

For the case where the inner-layer conductivity is 1.5 W/mK (the high value is chosen to illustrate our numerical solution method; in practice, one should not use such high-conductivity material for the inner layer), the present method yields an optimal outer-layer conductivity of 0.79 W/mK, compared with the ideal value of 2.6 W/mK based on Eq. (2). The close-to-ideal thermal-cloaking

performance of the optimized bilayer cloak is evident from the background isotherms shown in Fig. 3(c) and the low FOM in Table I. On the other hand, the background isotherms are visibly distorted for the analytical result based on the ideal solution, Fig. 3(d) (the distortion is a result of not satisfying the analytical assumption of a perfectly insulated inner layer in the bilayer theory). The corresponding FOM for the analytical solution is about  $3.87 \times 10^{-2}$  K. This case demonstrates the applicability of the present method to design bilayer thermal cloaks when the inner layer is made of realistic materials having low (but not zero) conductivity.

The ideal-bilayer solution in Ref. [10] can be readily extended to the case of a conducting inner layer. The corresponding analytical solution is reported here as an additional validation of the present numerical method:

$$\bar{\kappa} = \frac{-(1 + \gamma_1^2)(1 - g) \pm \sqrt{(1 + \gamma_1^2)^2(1 - g)^2 + 4g(\gamma_1^2 - 1)^2}}{2(1 - \gamma_1^2)}, \quad (7)$$

TABLE I. Validation of the method for a circular thermal cloak.

	$\kappa_2$ (W/mK)	$\kappa_b$ (W/mK)	$\eta$ (%)	$\lambda$ (K)	$\kappa_{\text{opt}}$ (W/mK)	$\kappa_{\text{bl}}$ (W/mK)
Case 1	0.001	10	0.04	$2.59 \times 10^{-8}$	25.99	26
Case 2	1.5	1	69.6	$1.89 \times 10^{-8}$	0.79	2.6



TABLE II. Validation of the method for an elliptical thermal cloak.

	$\kappa_2$ (W/mK)	$\kappa_b$ (W/mK)	$\eta$ (%)	$\lambda$ (K)	$\kappa_{\text{opt}}$ (W/mK)	$\kappa_{\text{bl}}$ (W/mK)
Case 1	0.001	10	0.25	$1.76 \times 10^{-5}$	24.39	24.45
Case 2	0.15	1	45.2	$1.02 \times 10^{-5}$	1.34	2.445

where  $g$  is a function of  $\bar{\kappa}_1$  and  $\bar{\kappa}_2$  only, and is given by

$$g = \frac{\bar{\kappa}_2 \gamma_2^2 (\bar{\kappa}_2 + \bar{\kappa}_1) - \bar{\kappa}_2 (\bar{\kappa}_2 - \bar{\kappa}_1)}{\gamma_2^2 (\bar{\kappa}_2 + \bar{\kappa}_1) + (\bar{\kappa}_2 - \bar{\kappa}_1)}, \quad (8)$$

and all conductivities are normalized with respect to the background conductivity  $\kappa_b$ .  $\bar{\kappa}_1$  is assumed to be 1 in all cases simulated in this work.  $\gamma_1$  and  $\gamma_2$  are defined as follows:

$$\gamma_1 = R_3/R_2 \text{ and } \gamma_2 = R_2/R_1. \quad (9)$$

Thus, for the case simulated,  $\bar{\kappa}_2 = 1.5$  and  $\bar{\kappa}_1 = 1$ . The corresponding value of  $\bar{\kappa}$  is 0.7898 from Eq. (7), in excellent agreement with the numerical optimization result.

The second validation case corresponds to a confocal elliptical bilayer thermal cloak [11]. The semimajor and semiminor axes of each elliptical boundary (denoted by elliptical coordinate  $\xi$ ) are 50 and 17.47 mm, respectively, for  $\xi_3$ , 48 and 10.44 mm, respectively, for  $\xi_2$ , and 46 and 8.44 mm, respectively, for  $\xi_1$ . The focal length  $p = 46.85$  mm for both  $\xi_3$  and  $\xi_2$  (confocal), while  $\xi_1$  is

not confocal. We chose a nonconfocal ellipse for the inner boundary of the inner layer to demonstrate the general purpose of our numerical procedure (not limited to confocal ellipses). Figure 4 shows the numerical results obtained by the present optimization method and by direct simulation using the ideal analytical solution, Eq. (3).

Table II summarizes the results and analyzed parameters. Similar conclusions as in the circular case can be drawn. In particular, for the case where the inner-layer conductivity is 0.001 W/mK, the present method again yields an optimal outer-layer conductivity in close agreement with the analytical value based on Eq. (3). For the case  $\kappa_2/\kappa_b = 0.15$ , the optimized cloak performs well, as indicated by the background isotherms shown in Fig. 4(c) and the low FOM. The ideal bilayer cloak yields distorted background isotherms as shown in Fig. 4(d) (the distortion is a result of not satisfying the analytical assumption of a perfectly insulated inner layer in the bilayer theory). The corresponding FOM is about  $1.56 \times 10^{-2}$  K.

As for the circular case, we remark that the ideal-bilayer solution in Ref. [11] may also be extended to the case of a conducting inner layer (i.e.,  $\kappa_2 \neq 0$ ), in principle. To

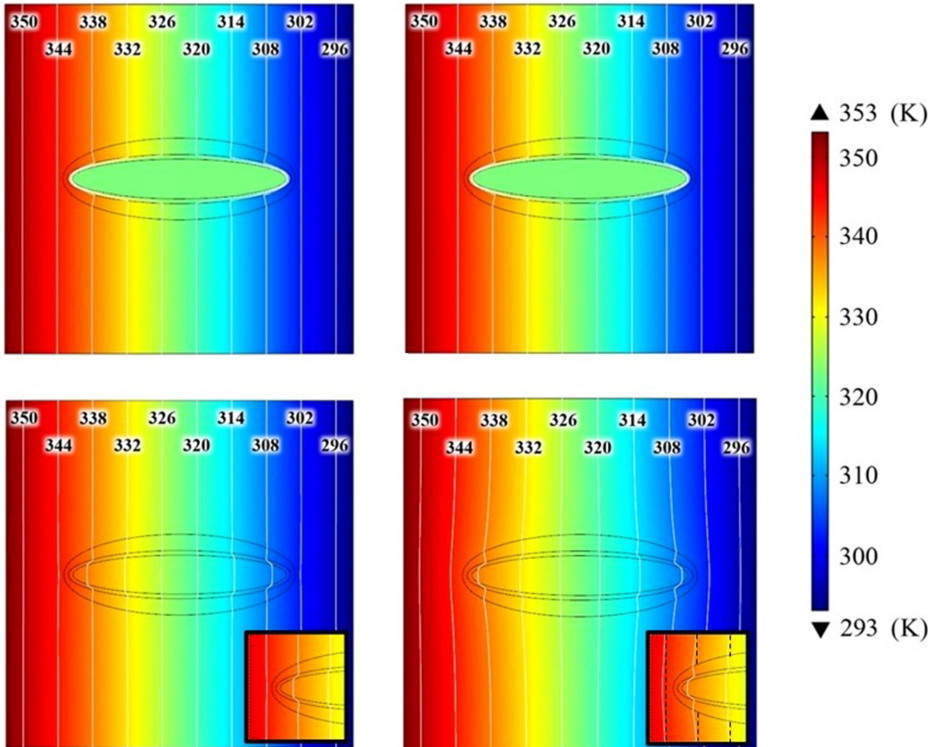


FIG. 4. Simulated temperature distributions around a confocal elliptical bilayer thermal cloak. (a),(b) Ideal conditions  $\kappa_2/\kappa_b = 10^{-4}$  in the inner layer and optimal thermal conductivity of the outer layer ( $\kappa_{\text{opt}} \approx 24.39$  W/mK) and ideal analytical solution for the thermal conductivity of the outer layer ( $\kappa = 24.45$  W/mK), respectively. (c),(d) Nonideal conditions  $\kappa_2/\kappa_b = 0.15$  in the inner layer and optimal thermal conductivity of the outer layer ( $\kappa_{\text{opt}} \approx 1.34$  W/mK) and ideal analytical solution for the thermal conductivity of the outer layer ( $\kappa = 2.445$  W/mK), respectively. White lines show isotherms and corresponding temperatures. Dashed black lines show the ideal cloaking isotherms.

generalize the analysis, the same system shown in Fig. 1 is used, with circles replaced by confocal ellipses. One then obtains six interface conditions at the three interfaces (continuity of temperature and normal heat flux), described by elliptical coordinate  $\xi_1$ ,  $\xi_2$ , and  $\xi_3$ , as follows:

$$E \cosh \xi_1 = A \cosh \xi_1 + B \sinh \xi_1, \quad (10)$$

$$\kappa_1 E \sinh \xi_1 = \kappa_2 (A \sinh \xi_1 + B \cosh \xi_1), \quad (11)$$

$$A \cosh \xi_2 + B \sinh \xi_2 = C \cosh \xi_2 + D \sinh \xi_2, \quad (12)$$

$$\kappa_2 (A \sinh \xi_2 + B \cosh \xi_2) = \kappa (C \sinh \xi_2 + D \cosh \xi_2), \quad (13)$$

$$C \cosh \xi_3 + D \sinh \xi_3 = t_0 \cosh \xi_3, \quad (14)$$

$$\kappa (C \sinh \xi_3 + D \cosh \xi_3) = \kappa_b t_0 \sinh \xi_3. \quad (15)$$

The coefficients  $A$ ,  $B$ ,  $C$ ,  $D$ , and  $E$  are associated with the general solution for the temperature fields in elliptical coordinates as follows:

$$T_4 = t_0 \cosh \xi \cos \eta, \quad (16)$$

$$T_3 = (C \cosh \xi + D \sinh \xi) \cos \eta, \quad (17)$$

$$T_2 = (A \cosh \xi + B \sinh \xi) \cos \eta, \quad (18)$$

$$T_1 = E \cosh \xi \cos \eta, \quad (19)$$

where subscripts 4, 3, 2, and 1 denote the background, the outer layer, the inner layer, and the cloaked region, respectively. The background temperature, Eq. (16), corresponds to a linear temperature distribution in  $x$  with gradient  $t_0$ , as usual. Solving the six interface conditions without assuming  $\kappa_2 = 0$ , we can show the solution for the unknown outer-layer conductivity  $\kappa$  to be

$$\frac{\bar{\kappa} \cosh^2 \xi_3 - \sinh^2 \xi_3}{(\bar{\kappa} - 1) \cosh \xi_3 \sinh \xi_3} = -\frac{D_a}{C_a}, \quad (20)$$

where

$$C_a = \bar{\kappa}_1 \sinh \xi_1 \left[ 1 + \frac{\bar{\kappa}_2 - \bar{\kappa}}{\bar{\kappa}_2} \frac{\sinh \xi_2 \sinh(\xi_2 - \xi_1)}{\sinh \xi_1} \right] - \bar{\kappa}_2 \sinh \xi_1 + (\bar{\kappa}_2 - \bar{\kappa}) \sinh \xi_2 \cosh(\xi_2 - \xi_1), \quad (21)$$

$$D_a = -\bar{\kappa}_2 \sinh \xi_2 \sinh(\xi_2 - \xi_1) + \bar{\kappa} \cosh \xi_2 \cosh(\xi_2 - \xi_1) - \frac{\bar{\kappa}_1}{\bar{\kappa}_2} \tanh \xi_1 \{ \bar{\kappa}_2 [\cosh \xi_1 \tanh \xi_2 + \tanh \xi_2 \sinh \xi_2 \sinh(\xi_2 - \xi_1)] - \bar{\kappa} \cosh \xi_2 \sinh(\xi_2 - \xi_1) \}. \quad (22)$$

Equation (20) represents a quadratic in the unknown  $\kappa$ , given all other conductivities. From the given ellipse dimensions,  $\xi_3$  and  $\xi_2$  are 0.365 and 0.221, respectively. The inner ellipse of the inner layer is not confocal, with  $\xi_1 \approx 0.186$ . For the case simulated,  $\bar{\kappa}_2 = 0.15$  and  $\bar{\kappa}_1 = 1$ . The corresponding value of  $\kappa$  is approximately 1.23 W/mK, in reasonable agreement with the optimized result of 1.34 W/mK. The difference is attributed to the ellipse  $\xi_1$  not being confocal with the bounding ellipses of the outer layer  $\xi_2$  and  $\xi_3$  in the physical system considered in the optimized solution.

Unlike the circular geometry, the ellipse is highly anisotropic geometrically. To demonstrate the general functionality of the proposed method, we present two more cases for the ellipse: the case when the heat flux is along the minor axis (for which the analytical bilayer solution is also available) and one oblique case when the heat flux is at  $30^\circ$  to the major axis (for which the analytical solution is not known). The thermal conductivities of the inner layer and the background are taken as  $\kappa_b = 10$  W/mK, and  $\kappa_2 = 0.001$  W/mK, respectively. Figure 5 shows the optimized results for the case when the heat flux is along the minor axis. The optimal conductivity is 200.44 W/mK, in perfect agreement with the analytical result of 200 W/mK determined from the analytical solution [note that the analytical solution for heat flux along the minor axis is given by  $\kappa = \tanh \xi_2 \tanh(\xi_2 - \xi_1)$  [11]]. The optimization results for the oblique-heat-flux case are shown in Fig. 6(a), where the optimal outer-layer conductivity is computed as 46.89 W/mK and the corresponding FOM,  $\lambda$ , is approximately  $7.26 \times 10^{-2}$  K. As can be seen, even with the optimal outer-layer conductivity, the performance of the particular elliptical bilayer cloak considered in the validation study may be inadequate. These results do not invalidate our method; they simply point out that, within the confines

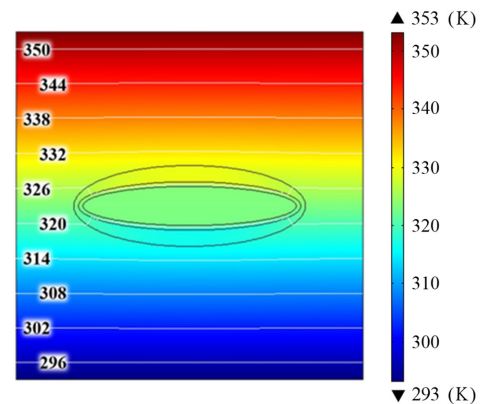


FIG. 5. Simulated temperature distributions around a confocal elliptical bilayer thermal cloak with heat flux along the minor axis. The optimal outer-layer thermal conductivity  $\kappa_{\text{opt}}$  is approximately 200.44 W/mK. White lines show isotherms and corresponding temperatures.

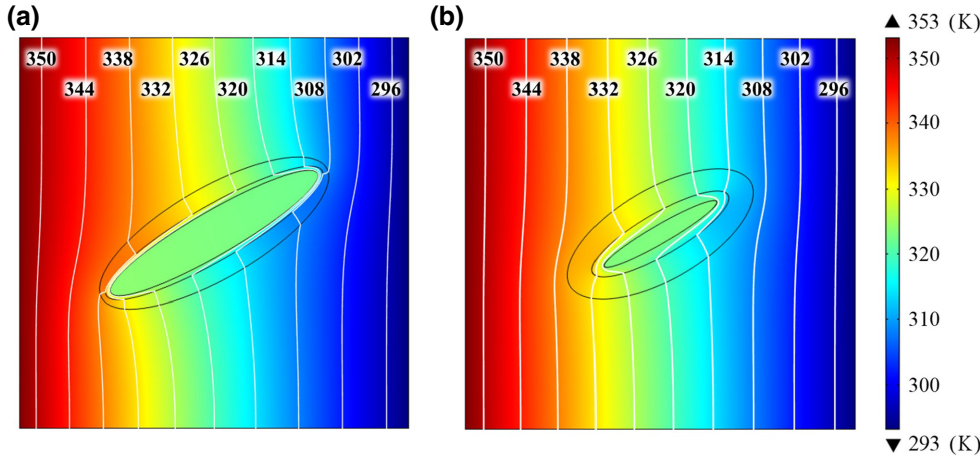


FIG. 6. Simulated temperature distribution for an elliptical bilayer thermal cloak with heat flux at  $30^\circ$  to the major axis. (a) Original elliptical bilayer cloak as in Fig. 4. (b) Redesigned elliptical bilayer thermal cloak. White lines denote isotherms at indicated temperatures.

of the simple bilayer theory, some designs perform better than others depending on the cloak geometry and the background thermal fields. To this end, we redesign an elliptical bilayer cloak as shown in Fig. 6(b). The semi-major and semiminor axes of each elliptical boundary are 40 and 17.47 mm, respectively, for  $\xi_3$ , 30 and 8 mm, respectively, for  $\xi_2$ , and 25 and 3.47 mm, respectively, for  $\xi_1$ . The ellipses in the new design are nonconfocal. The optimization method yields an optimal outer-layer thermal conductivity of approximately 23.72 W/mK, and the corresponding FOM,  $\lambda$ , is about  $2.83 \times 10^{-2}$  K. The optimization results in Fig. 6(b) show that the background isotherms are less distorted compared with the results in Fig. 6(a) from the geometry redesign. This suggests that our method can be used to improve the design of a bilayer thermal cloak if the given design does not yield an adequate cloaking performance.

In summary, the results presented in Figs. 3–5 confirm the accuracy of the present method by successfully reproducing the analytical results when the inner layer is ideally insulated. For situations where the inner layer is not perfectly insulated, or when the system deviates from the analytical condition (e.g., nonconfocal boundaries, or oblique heat-flux direction, for elliptical cloaks), our method yields an optimal outer-layer conductivity that will result in the best-possible thermal-cloaking performance, even though this best-possible performance may not be desirable from a practical standpoint.

#### IV. BILAYER THERMAL CLOAKS WITH ARBITRARY GEOMETRY

Having validated our method against known analytical solutions, we now expand our study to consider bilayer cloaks with arbitrary shapes. For all shapes considered, the thermal conductivity of the inner layer and the background are taken as  $\kappa_2 = 0.15$  W/mK and  $\kappa_b = 10$  W/mK, respectively.

#### A. Square bilayer cloak

We consider a square bilayer thermal cloak with a square protected region of side  $a = 10$  mm. Four different cases are simulated. Cases 1 and 2 correspond to an inner layer of side  $b = 25$  mm and an outer layer of side  $c = 40$  mm. Cases 3 and 4 correspond to  $b = 15$  mm and  $c = 40$  mm. For each cloak, a layer-thickness ratio  $\sigma = (c - b)/b - a$  is defined to indicate the relative proportions of the inner and outer layers. Moreover, to investigate the effect of the sharp corners of the thermal cloak on the temperature distribution, the simulations consider two different rotation angles of the background heat flow—namely,  $\alpha = 0^\circ$  and  $45^\circ$  (see Table III).

Figures 7(a) and 7(b) show the simulation results for cases 1 and 2. The initial values of  $\kappa_0$  and  $\kappa_1$  are set as 20 and 30 W/mK, respectively, on the basis of an effective area of 22.82 W/mK from Eq. (6). The optimization process converges within five iterations. Figures 7(c) and 7(d) present the simulation results for cases 3 and 4. The initial values of  $\kappa_0$  and  $\kappa_1$  are set as 10 and 20 W/mK, respectively, on the basis of an effective area of 13.27 W/mK. The optimization method converges within seven iterations. The results for the optimal outer-layer conductivity are summarized in Table III. The results show that the optimal outer-layer conductivity is relatively independent of the heat-flux direction. Also a thick outer layer performs better (in terms of cloaking) than the thin counterpart [Figs. 7(a) and 7(c)]. In both designs, the cloak

TABLE III. Simulation cases and results for square bilayer thermal cloaks with different layer-thickness ratios and background rotation angles.

	$\sigma$	$\alpha$ (deg)	$\lambda$ (K)	$\kappa_{\text{opt}}$ (W/mK)
Case 1	1	0	$3.37 \times 10^{-3}$	24.68
Case 2	1	45	$4.25 \times 10^{-3}$	24.71
Case 3	5	0	$1.21 \times 10^{-3}$	13.45
Case 4	5	45	$1.43 \times 10^{-3}$	13.45

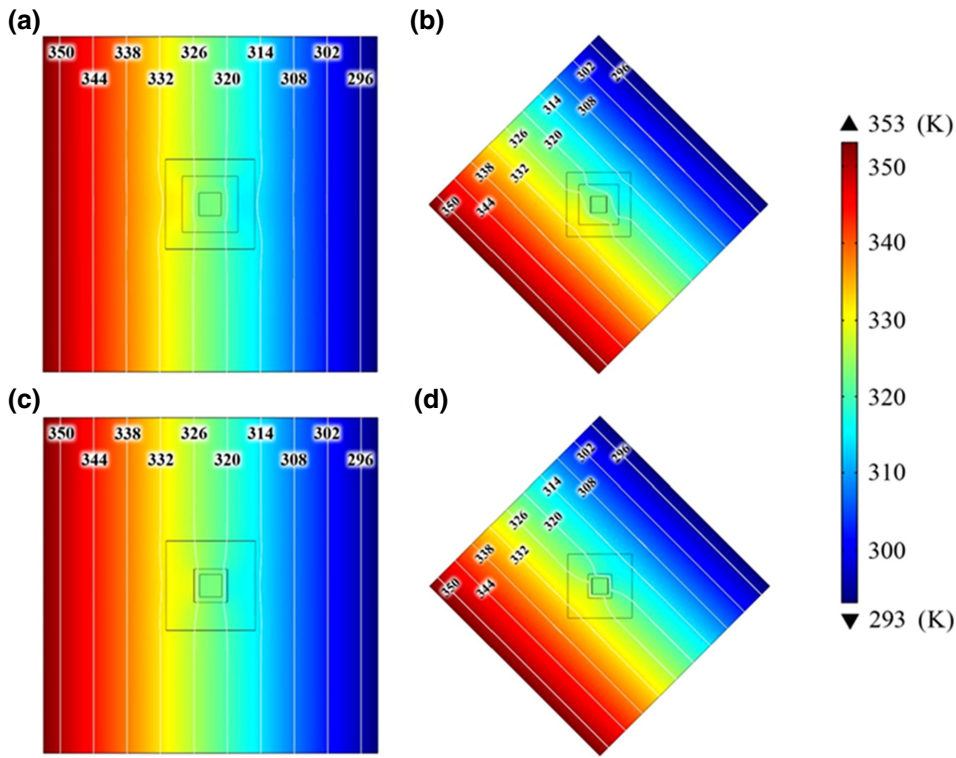


FIG. 7. Simulated temperature distributions for square bilayer thermal cloaks with different layer-thickness ratios  $\sigma$  and heat-flow angles  $\alpha$ . (a)  $\sigma = 1$  and  $\alpha = 0^\circ$  (case 1). (b)  $\sigma = 1$  and  $\alpha = 45^\circ$  (case 2). (c)  $\sigma = 5$  and  $\alpha = 0^\circ$  (case 3). (d)  $\sigma = 5$  and  $\alpha = 45^\circ$  (case 4). White lines denote the isotherms and corresponding temperatures.

performs better when the heat-flow direction is not normal to the side of the square, as indicated by the almost-straight isotherms [Figs. 7(b) and 7(d)]. In general, distortion of the background temperature field is expected near the sharp corners of a square cloak. However, as the relative thickness of the outer layer increases, distortions produced by the sharp corners appear to be significantly reduced. From Table III, it is seen that for the same rotation angle, a greater layer-thickness ratio  $\sigma$  results in both a lower average temperature deviation  $\lambda$  and a lower optimal thermal conductivity of the outer layer  $\kappa_{\text{opt}}$ .

### B. Diamond-shaped bilayer cloak

A multilayered diamond-shaped thermal cloak consisting of a large number of alternating layers of four homogeneous and isotropic natural materials has been proposed [19]. Here we investigate the performance of a bilayer diamond-shaped thermal cloak having the same outer dimension as in Ref. [19]. In the simulations, the short and long diagonal lengths of the protected region are specified as 20 and 40 mm, respectively. In addition, the diagonal lengths of the inner layer are set as 24 and 48 mm, respectively, while those of the outer layer are both set as 80 mm. The initial values of  $\kappa_0$  and  $\kappa_1$  are set as 10 and 20 W/mK, respectively, on the basis of an effective area of 14.39 W/mK from Eq. (6).

Figure 8 presents the optimized results obtained for the simplified bilayer-cloak structure. For a horizontal heat flow, the optimization method converges within seven

iterations and yields an optimal outer-layer thermal conductivity of 12.57 W/mK. The average temperature deviation,  $\lambda$ , is about  $1.49 \times 10^{-3}$  K. For a vertical heat flow, the optimization method requires four iterations to converge and yields an optimal outer-layer thermal conductivity of 18.55 W/mK, with an average temperature deviation of  $4.97 \times 10^{-3}$  K. In contrast to the square bilayer thermal cloak, the optimal outer-layer thermal conductivity for the diamond-shaped thermal cloak changes with the heat-flow angle since the diamond geometry is not geometrically isotropic relative the diagonals. In particular, when the direction of the heat flow is perpendicular to the long diagonal of the cloak, the thermal conductivity increases significantly. When compared with the multilayered structure in Ref. [19], the diamond-shaped bilayer cloak has comparable thermal-cloaking performance. Thus, the present results demonstrate that the simpler bilayer design performs comparably to the multilayered design.

### C. Asymmetric irregular thermal cloak

The thermal cloaks considered so far (circular, elliptical, square, and diamond shaped) have a regular geometric form. To further demonstrate the practical applicability of the proposed optimization method, a thermal cloak with the asymmetric irregular form shown in Fig. 9 is considered, which is similar to that studied in Ref. [20]. The boundary of the cloak is a closed curve defined by the continuous periodic function  $f(\theta) = 1 + 0.3 \cos 3\theta$ ,  $0 \leq \theta \leq 2\pi$ . The radius of the protected region is  $10f(\theta)$



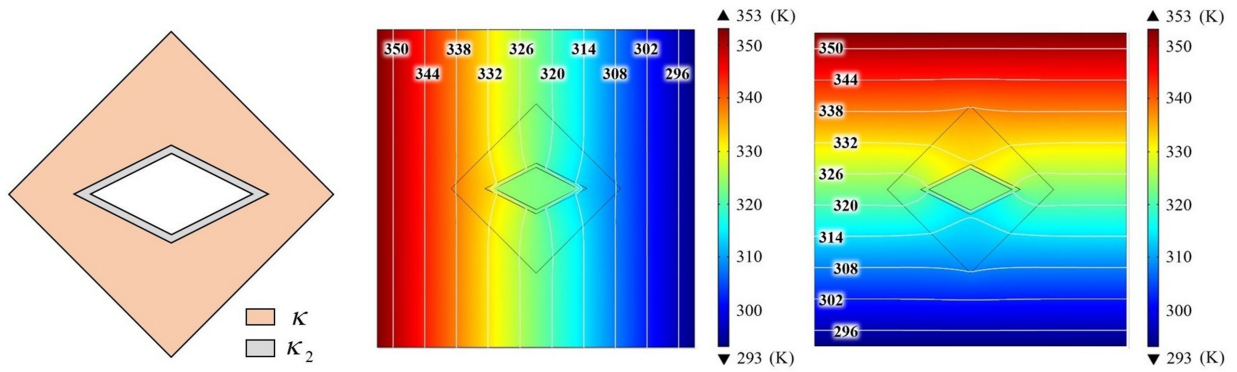


FIG. 8. Diamond-shaped bilayer thermal cloak considered in the present study. The left panel shows an illustration of the structure of the thermal cloak. The middle panel and the right panel show the cloaking performance of cloaks for horizontal and vertical heat flows, respectively. White lines denote isotherms and corresponding temperatures.

mm, while the radii of the inner and outer layers of the cloak are  $11f(\theta)$  mm and  $30f(\theta)$  mm, respectively. The background heat flow is in the horizontal direction. The optimization yields an optimal outer-layer thermal conductivity of approximately 13.15 W/mK, and the average temperature deviation is approximately  $4.14 \times 10^{-3}$  K. Figure 9 shows the optimized results. It can be seen that the isotherms undergo only slight distortion outside the protected region. The effectiveness of the designed bilayer cloak is confirmed.

#### D. Space-capsule-shaped bilayer thermal cloak

To further test the method on an arbitrary shape, we consider a geometry with an aperiodic boundary. We design a space-capsule-shaped cloak as shown in Fig. 10. To demonstrate the generality of our method, we use different thicknesses for the outer layer. For the case simulated, the

thickness of the left, curved side is 35 cm, and that of the rest of outer layer is set as 25 cm. The thickness of inner layer is uniform at 10 cm. The background heat flow is in the horizontal direction. The optimization method yields an optimal outer-layer thermal conductivity of approximately 33.7 W/mK, and the average temperature deviation,  $\lambda$ , is about  $4.76 \times 10^{-3}$  K. Figure 10 shows the optimized results. It can be seen that the isotherms near the boundary of the cloak are slightly distorted. The results demonstrate that the optimization method can be applied to cloaks with a discontinuous aperiodic shape, as expected.

#### V. NONLINEAR BACKGROUND TEMPERATURE DISTRIBUTION

Our method does not depend on the background temperature distribution. The cases considered so far all assume

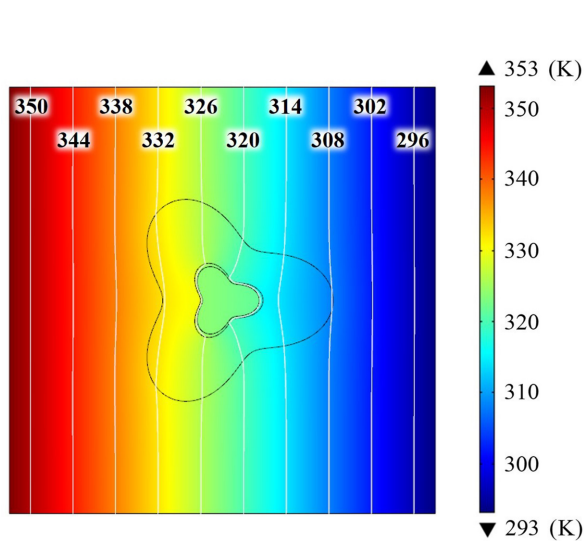


FIG. 9. Simulated temperature distribution for an irregular bilayer thermal cloak. White lines denote isotherms and corresponding temperatures.

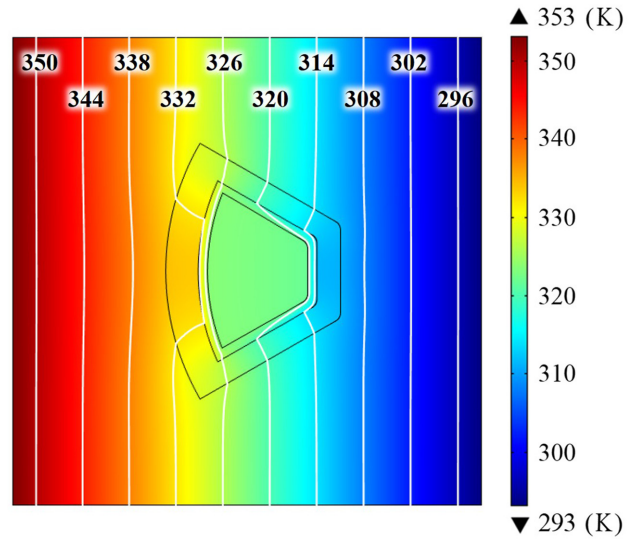


FIG. 10. Simulated temperature distribution for a space-capsule-shaped bilayer thermal cloak. White lines denote isotherms and corresponding temperatures.

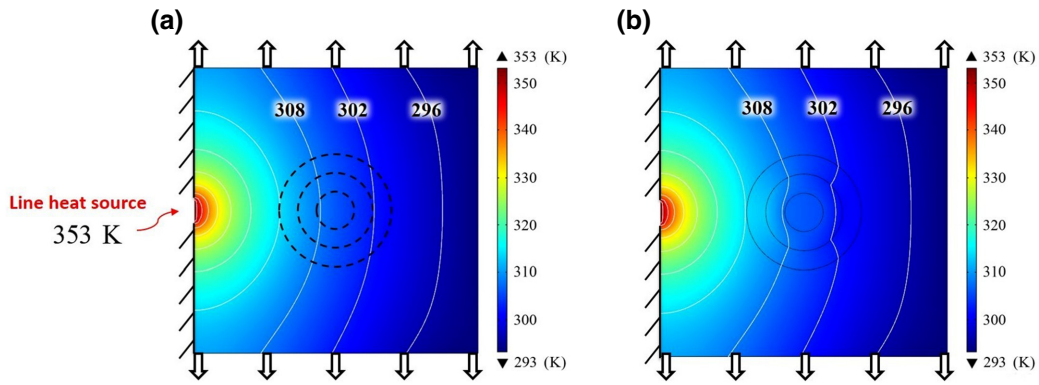


FIG. 11. Simulated temperature distributions for a circular bilayer thermal cloak used in a background temperature field with a nonlinear distribution. (a) Pure background (no thermal cloaking device). (b) Thermal cloaking device with outer layer having optimal thermal conductivity of approximately 2.15 W/mK. White lines denote isotherms and corresponding temperatures.

a linear background temperature distribution for simplicity. In many practical applications, the background temperature distribution may indeed be nonlinear. Accordingly, we conclude the present study by investigating the thermal-cloaking performance of a circular bilayer cloak in a nonlinear temperature field due to the presence of a line heat source. The dimensions of the model are assumed to be the same as those considered for the circular thermal cloak in Sec. III. In the simulation, the line source has a length of 10 mm and a temperature of 353 K and is located at the center of the left boundary, with the remaining boundary insulated. The right boundary is maintained at a constant low temperature of 293 K, and the upper and lower boundaries are assumed to experience heat loss proportional to the local temperature at a rate of  $qT$ , with  $q$  set as  $0.3 \text{ W/m}^2 \text{ K}$ . In the absence of the cloak, the isotherms are distributed in the radial direction, as shown in Fig. 11(a). The optimization method yields an optimal outer-layer conductivity of 2.15 W/mK. Figure 11(b) shows the isotherms with the bilayer-cloak system. The isotherm distribution is almost the same as that for the pure-background case, indicating good cloaking performance. The average temperature deviation is about  $2.39 \times 10^{-3} \text{ K}$ . The results demonstrate the applicability of the proposed method to a nonlinear background temperature distribution.

## VI. CONCLUSIONS

An optimization method based on an inverse approach for the design of planar arbitrary-geometry bilayer thermal cloaks is presented. The method is based on the bilayer theory [10,11] and avoids the need for anisotropic thermal metamaterials [6,20] or multilayer discrete structures [7,9,21]. In particular, the optimal conductivity for the outer layer of the bilayer cloak is determined, yielding the best-possible cloaking performance by minimally impacting the given background temperature distribution. The method

relaxes the requirement of a perfectly insulated inner layer, which is deemed difficult to fabricate in practice. To this end, the analytical solutions for a circular bilayer cloak and a confocal elliptical bilayer cloak with a conducting inner layer are also derived and presented. We validate our method against known analytical solutions; excellent agreement with analytical results is obtained (including the general case of a conducting inner layer). The general applicability of the proposed method is demonstrated by numerical results. Various cloak geometries, including circular, elliptical, square, and diamond shaped, as well as geometries with nonuniform and asymmetric contours are considered. The cloaking effectiveness of the bilayer design ultimately depends on the shape chosen. In other words, one can always find an optimized solution (such that the cost function achieves a minimum value), but the resulting cloaking effectiveness of the bilayer cloak may be less than desirable (with regard to not impacting the background temperature field.) Overall, the results establish that the proposed method provides an effective approach for the design of a bilayer thermal cloak of arbitrary shape. The method can also be applied to a nonlinear background temperature distribution. Future studies may usefully extend the proposed method to thermal cloaking problems involving thermal convection [22,23] and radiation [24].

## ACKNOWLEDGMENTS

This study was supported by grants from Taiwan Ministry of Science and Technology (MOST): Grants No. MOST-108-2811-E-006-500 (W.-S.Y.) and No. MOST-107-2221-E-006-126-MY3 (R.-J.Y.).

- [1] E. M. Dede, F. Zhuo, P. Schmalenberg, and T. Nomura, Thermal metamaterials for heat flow control in electronics, *J. Electron. Packag.* **140**, 010904 (2018).

- [2] U. Leonhardt, Optical conformal mapping, *Science* **312**, 1777 (2006).
- [3] J. B. Pendry, D. Schurig, and D. Smith, Controlling electromagnetic fields, *Science* **312**, 1780 (2006).
- [4] C. Z. Fan, Y. Gao, and J. P. Huang, Shaped graded materials with an apparent negative thermal conductivity, *Appl. Phys. Lett.* **92**, 251907 (2008).
- [5] T. Y. Chen, C.-N. Weng, and J.-S. Chen, Cloak for curvilinearly anisotropic media in conduction, *Appl. Phys. Lett.* **93**, 114103 (2008).
- [6] S. Guenneau, C. Amra, and D. Veynante, Transformation thermodynamics: Cloaking and concentrating heat flux, *Opt. Express* **20**, 8207 (2012).
- [7] S. Narayana and Y. Sato, Heat Flux Manipulation with Engineered Thermal Materials, *Phys. Rev. Lett.* **108**, 214303 (2012).
- [8] M. Wang, S. Huang, R. Hu, and X. Luo, Analysis of elliptical thermal cloak based on entropy generation and entransy dissipation approach, *Chin. Phys. B* **28**, 087804 (2019).
- [9] B. He, W. Yang, and F. Liu, The material parameter design and finite element simulation of the quadrilateral thermal cloak device, *Appl. Math. Lett.* **94**, 99 (2019).
- [10] T. Han, X. Bai, D. Gao, J. T. L. Thong, B. Li, and C.-W. Qiu, Experimental Demonstration of a Bilayer Thermal Cloak, *Phys. Rev. Lett.* **112**, 054302 (2014).
- [11] T. Han, P. Yang, Y. Li, D. Lei, B. Li, K. Hippalgaonkar, and C. Qiu, Full? parameter omnidirectional thermal metadivices of anisotropic geometry, *Adv. Mater.* **30**, 1804019 (2018).
- [12] W.-S. Yeung, F.-Y. Yang, and R.-J. Yang, Analysis of a trilayer thermal cloak, *AIP Adv.* **10**, 055102 (2020).
- [13] Y. Li, K. J. Zhu, Y. G. Peng, W. Li, T. Yang, H. X. Xu, H. Chen, X. F. Zhu, S. Fan, and C. W. Qiu, Thermal meta-device in analogue of zero-index photonics, *Nat. Mater.* **18**, 48 (2019).
- [14] J. Qin, W. Luo, P. Yang, B. Wang, T. Deng, and T. Han, Experimental demonstration of irregular thermal carpet cloaks with natural bulk material, *Int. J. Heat Mass Transf.* **141**, 487 (2019).
- [15] G. Alekseev and D. Tereshko, Optimization-based method of solving 2d thermal cloaking problems, *J. Phys. Conf. Ser.* **1268**, 012004 (2019).
- [16] W. Gautschi, *Numerical Analysis* (Springer Science & Business Media, New York, 1997).
- [17] COMSOL Multiphysics<sup>®</sup> (COMSOL AB, Sweden) <https://www.comsol.com>.
- [18] MATLAB<sup>®</sup> (Mathworks, Framingham, Massachusetts, USA) <https://www.mathworks.com>.
- [19] T.-H. Li, D.-L. Zhu, F.-C. Mao, M. Huang, J.-J. Yang, and S.-B. Li, Design of diamond-shaped transient thermal cloaks with homogeneous isotropic materials, *Front. Phys.* **11**, 110503 (2016).
- [20] T. Yang, L. Huang, F. Chen, and W. Xu, Heat flux and temperature field cloaks for arbitrarily shaped objects, *J. Phys. D* **46**, 305102 (2018).
- [21] Y. Liu, W. Guo, and T. Han, Arbitrarily polygonal transient thermal cloaks with natural bulk materials in bilayer configurations, *Int. J. Heat Mass Transf.* **115**, 1 (2017).
- [22] G. Dai, J. Shang, and J. Huang, Theory of transformation thermal convection for creeping flow in porous media: Cloaking, concentrating, and camouflage, *Phys. Rev. E* **97**, 022129 (2018).
- [23] W.-S. Yeung, V.-P. Mai, and R.-J. Yang, Cloaking: Controlling Thermal and Hydrodynamic Fields Simultaneously, *Phys. Rev. Appl.* **13**, 064030 (2020).
- [24] L. Xu and J. Huang, Metamaterials for Manipulating Thermal Radiation: Transparency, Cloak, and Expander, *Phys. Rev. Appl.* **12**, 044048 (2019).